Circulation: Arrhythmia and Electrophysiology

ORIGINAL ARTICLE

Preclinical Study of Pulsed Field Ablation of Difficult Ventricular Targets: Intracavitary Mobile Structures, Interventricular Septum, and Left Ventricular Free Wall

Moritz Nies, MD; Keita Watanabe, MD; Iwanari Kawamura, MD; Carlos G. Santos-Gallego, MD; Vivek Y. Reddy, MD; Jacob S. Koruth, MD

BACKGROUND: Endocardial catheter-based pulsed field ablation (PFA) of the ventricular myocardium is promising. However, little is known about PFA's ability to target intracavitary structures, epicardium, and ways to achieve transmural lesions across thick ventricular tissue.

METHODS: A lattice-tip catheter was used to deliver biphasic monopolar PFA to swine ventricles under general anesthesia, with electroanatomical mapping, fluoroscopy and intracardiac echocardiography guidance. We conducted experiments to assess the feasibility and safety of repetitive monopolar PFA applications to ablate (1) intracavitary papillary muscles and moderator bands, (2) epicardial targets, and (3) bipolar PFA for midmyocardial targets in the interventricular septum and left ventricular free wall.

RESULTS: (1) Papillary muscles (n=13) were successfully ablated and then evaluated at 2, 7, and 21 days. Nine lesions with stable contact measured 18.3±2.4 mm long, 15.3±1.5 mm wide, and 5.8±1.0 mm deep at 2 days. Chronic lesions demonstrated preserved chordae without mitral regurgitation. Two targeted moderator bands were transmurally ablated without structural disruption. (2) Transatrial saline/carbon dioxide assisted epicardial access was obtained successfully and epicardial monopolar lesions had a mean length, width, and depth of 30.4±4.2, 23.5±4.1, and 9.1±1.9 mm, respectively. (3) Bipolar PFA lesions were delivered across the septum (n=11) and the left ventricular free wall (n=7). Twelve completed bipolar lesions had a mean length, width, and depth of 29.6±5.5, 21.0±7.3, and 14.3±4.7 mm, respectively. Chronically, these lesions demonstrated uniform fibrotic changes without tissue disruption. Bipolar lesions were significantly deeper than the monopolar epicardial lesions.

CONCLUSIONS: This in vivo evaluation demonstrates that PFA can successfully ablate intracavitary structures and create deep epicardial lesions and transmural left ventricular lesions.

GRAPHIC ABSTRACT: A graphic abstract is available for this article.

Key Words: catheter ablation ■ electroporation ■ heart ventricles ■ papillary muscles ■ swine ■ tachycardia, ventricular

Ventricular arrhythmia ablation continues to have suboptimal long-term success rates, partly related to limitations of currently used ablative energies, which is typically radiofrequency current.[1–3] Creating deep lesions for intramural targets, ablating mobile intracavitary structures, and penetrating scarred myocardium

Correspondence to: Jacob S. Koruth, MD, Helmsley Electrophysiology Center, Mt Sinai Fuster Heart Hospital, Department of Cardiology, Icahn School of Medicine at Mt Sinai, One Gustave L. Levy Pl, Box 1030, New York, NY 10029. Email jacob.koruth@mountsinai.org
Supplemental Material is available at https://www.ahajournals.org/doi/suppl/10.1161/CIRCEP.124.012734.
For Sources of Funding and Disclosures, see page 352.

WHAT IS KNOWN?

- Ventricular ablation has suboptimal success rates due to limited lesion depth with radiofrequency ablation, especially for mobile intracavitary structures like papillary muscles and deep myocardial substrates.
- The application of endocardial pulsed field ablation in the ventricles currently has limited lesion depth and is unable to achieve transmural left ventricular ablation.

WHAT THE STUDY ADDS

- Monopolar pulsed field ablation with the lattice-tip catheter can create reliable, high-quality lesions on papillary muscles and moderator bands, without disruption of these difficult to ablate structures.
- Monopolar epicardial pulsed field ablation with the same tip can create deep and wide lesions, and catheter-tip to catheter-tip bipolar pulsed field ablation facilitates transmural left ventricular ablation.

Nonstandard Abbreviations and Acronyms

ICE	intracardiac echocardiography
LV	left ventricle
MRI	magnetic resonance imaging
PFA	pulsed field ablation
PM	papillary muscle
RV	right ventricle
VF	ventricular fibrillation

are instances where radiofrequency current is known to be challenging or even ineffective.[4–9] Several approaches have been developed to overcome this, such as the use of long-duration, half-normal saline irrigation, and bipolar approaches to radiofrequency ablation, in addition to using other energy sources such as cryoablation, radioablation, and alcohol ablation.[10–16]

Pulsed field ablation (PFA) has recently been recognized for its potential to improve both the efficacy and safety of atrial ablation procedures.[17–20] Its nonthermal basis of ablation, reduced reliance on prolonged high-quality contact, and short delivery times also make it relevant for ventricular ablation, and early preclinical studies have been promising.[21–25] However, PFA's ability to make deeper and larger lesions than radiofrequency current, as well as creating adequate lesions on mobile intracavitary structures such as the papillary muscles (PMs) and moderator band has yet to be determined.[26–29] This preclinical report specifically explores the ability of PFA to target mobile intracavitary structures and details the efficacy and safety of several strategies to maximize ventricular ablation using pulsed fields via a large catheter tip form factor that favors stability.

METHODS

Data and methods used in the analysis and materials used to conduct the research will not be available for access. All experiments were approved by the Institutional Animal Care and Use Committee at the Mount Sinai Hospital, New York. A total of 14 Yorkshire swine (5 female, 9 male) were included in this study. Predetermined survival periods were 2 days (n=10), 7 days (n=2), and 21 days (n=2). Based on prior experience, we elected to use 10 animals in the 2-day survival group to accommodate all ablation targets. We aimed to use a minimum of 3 animals for each ablation target to ensure an adequate number of lesions for analysis. As this feasibility study also focused on safety, 4 animals with longer survival periods (7 and 21 days) were included to evaluate the structural and functional integrity of ablated PMs and bipolar lesion sites.

Ablation System and Preclinical Workflow

The deflectable, lattice-tip catheter (Sphere-9; Medtronic, Minneapolis, MN) facilitates 3-dimensional mapping (Affera Mapping System; Medtronic) and ablation via a PFA generator (HexaPulse; Medtronic), as previously described.[30,31] Monopolar PFA is delivered from the entire lattice tip using a proprietary, biphasic waveform.[30,31] Under general anesthesia, after transfemoral venous access, the ablation catheter was placed in the right ventricle (RV) or left ventricle (LV) using a deflectable sheath, or both (Agilis; Abbott, Chicago, IL). Transeptal or retrograde aortic access was used for endocardial catheter placement in the LV. For epicardial catheter placement, subxiphoid access was obtained after transatrial epicardial carbon dioxide (CO_2) insufflation or saline injection: after advancing a 6F guiding catheter (JCL3.0; Medtronic) to the tip of the right atrial appendage, the right atrial appendage was punctured using a 1.9 Fr coronary microcatheter (Caravel; Asahi Intecc, Irvine, CA) and a 0.014" angioplasty wire (Hi-Torque Whisper ES; Abbott). The microcatheter was then advanced over the wire into the pericardial space, and insufflation with CO_2 or saline injection was performed to separate the pericardial layers. After a subsequent standard subxiphoid puncture, the lattice-tip catheter was placed in the epicardial space through a short, deflectable sheath (Agilis; Abbott).

An activated clotting time of 300 to 400 seconds was targeted for all procedures. Catheter position and stability were carefully monitored using intracardiac echocardiography (ICE), fluoroscopy, and electroanatomic mapping. Two specific experiments were performed, each designed to address different challenges encountered during ventricular ablation:

Intracavitary Structure Ablation

LV, RV PMs, and RV moderator bands were identified using ICE. Once catheter tip contact was ensured, ablation was performed by repetitive (3–5) deliveries of 5.5-second long applications with a minimum time interval of 7 to 8 seconds between applications (Figures 1 through 3). During applications, 2 observers (J.S.K. and M.N.) adjudicated quality of contact using ICE with careful annotation of instances of intermittent contact.

Epicardial and Bipolar Ablation

Two different ablation approaches were evaluated: (1) epicardial monopolar PFA using 4 to 5 repetitive applications of the 5.5-second dose, as previously described (Figure 4).[23] We

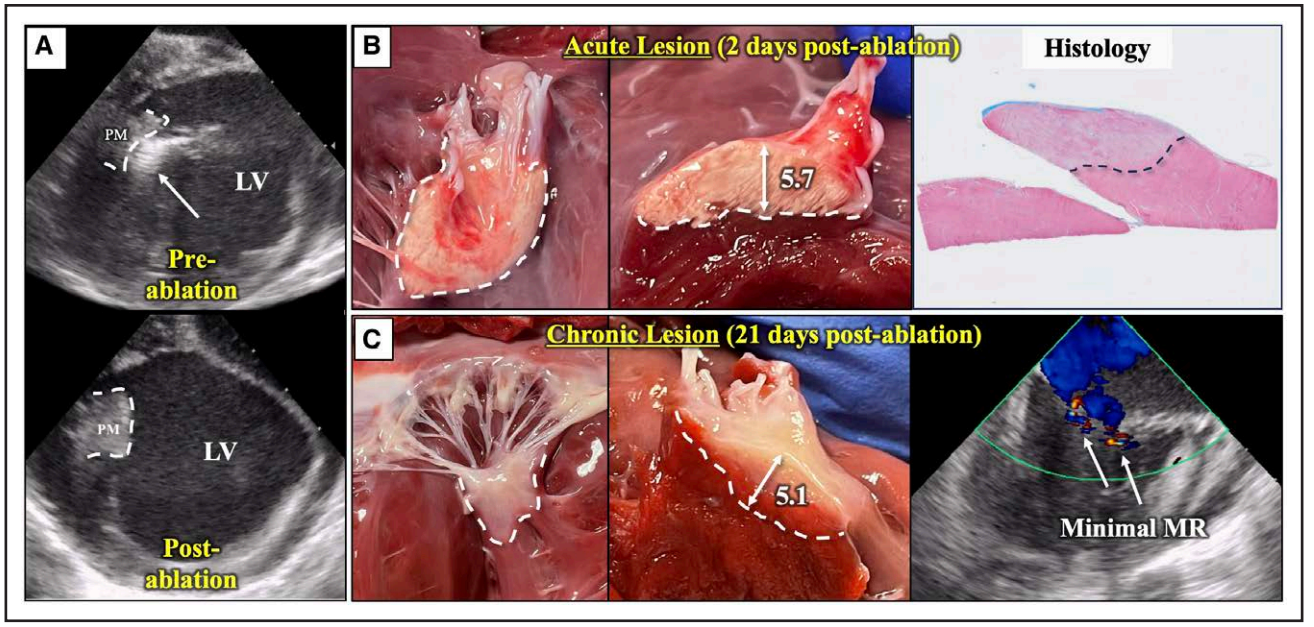

Figure 1. Papillary muscle (PM) ablation.
A, Intracardiac echocardiography (ICE) images. **Top**, Catheter tip (arrow) in contact with the left ventricular (LV) posterior PM before ablation. **Bottom**, ICE image 90 minutes post-ablation with echogenic changes. **B**, Necropsy and histology findings 2 days post-ablation. Lesion confined to the PM. A small area of hemorrhage is seen. Maximum lesion depth was 5.7 mm. Histology (Masson Trichrome) reveals homogeneous necrosis (dotted line). **C**, After 21 days of survival, the PMs retain their integrity and overall structure. Chordae were intact (**left**) with a maximum lesion depth of 5.1 mm. There was no significant mitral valve regurgitation noted on ICE. MR indicates mitral regurgitation.

avoided the base of the ventricles and the septal epicardium (to avoid the main coronary arteries) and marked locations using the mapping system. (2) Bipolar ablation using 2 catheter tips across ventricular myocardial tissue (interventricular septum or LV free wall; Figures 5 through 7). For bipolar ablation, a second ablation catheter was connected to the PF generator's grounding channel, thereby functioning as the return electrode. Similar to bipolar radiofrequency ablation, the catheter tips were placed on opposite sides of the targeted ventricular wall using ICE and fluoroscopic guidance. Ablation was then performed via repeated (4–7) deliveries of 5.5-second applications. The tips were purposefully offset to each other to different degrees to allow for assessment of maximum achievable depth (Figure 5). This was done to explore the capacity of this approach to achieve transmurality across different separation distances. In 2 animals, cardiac magnetic resonance imaging (MRI) was performed with a 3.0 Tesla magnet (Sonata Magneton, Siemens) using previously described protocols.[24]

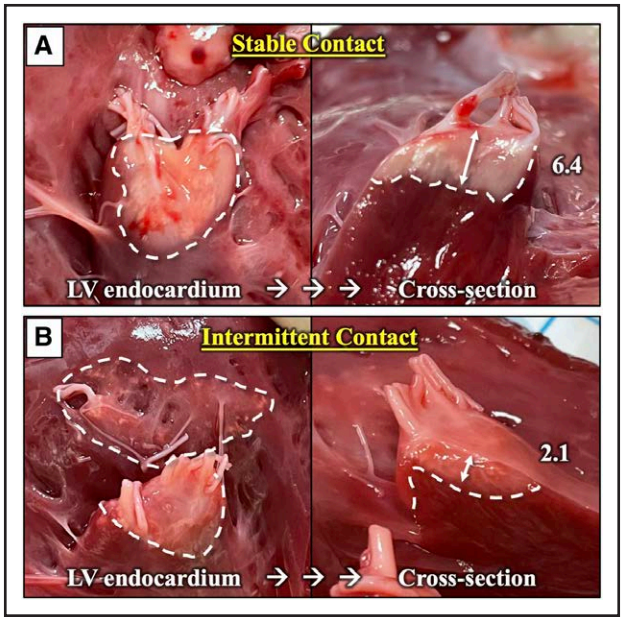

Figure 2. Papillary muscle (PM) ablation, effect of tissue contact.
A, PM lesion (dotted line) 2 days post-ablation with good, stable contact. The lesion is confined to the PM and achieved a maximum depth of 6.4 mm. **B**, PM ablation with intermittent contact with wider but shallower (2.1 mm depth) lesion, extending to neighboring myocardium. LV indicates left ventricle.

Pathological Evaluation

After completion of the survival period, animals were humanely euthanized using pentobarbital. The chest was opened, and thoracic organs were inspected and photographed. Tetrazolium trichloride was perfused and the heart was opened. Lesions were identified and then fixed in 10% buffered formalin for further analyses. Incomplete lesions were excluded from dimension analyses and comparisons. Lesions were sectioned, measured, and photographed. The samples were embedded in paraffin, cut to 2 slides each, and stained with hematoxylin and eosin and Masson Trichrome, respectively. Slides were reviewed by board-certified veterinary pathologists who were blinded to electroanatomic data and outcomes. Microscopic measurements were taken with histopathologist analysis of the lesion border and measured on a transverse plane, originating from the assumed point of tissue contact with the ablation catheter tip.

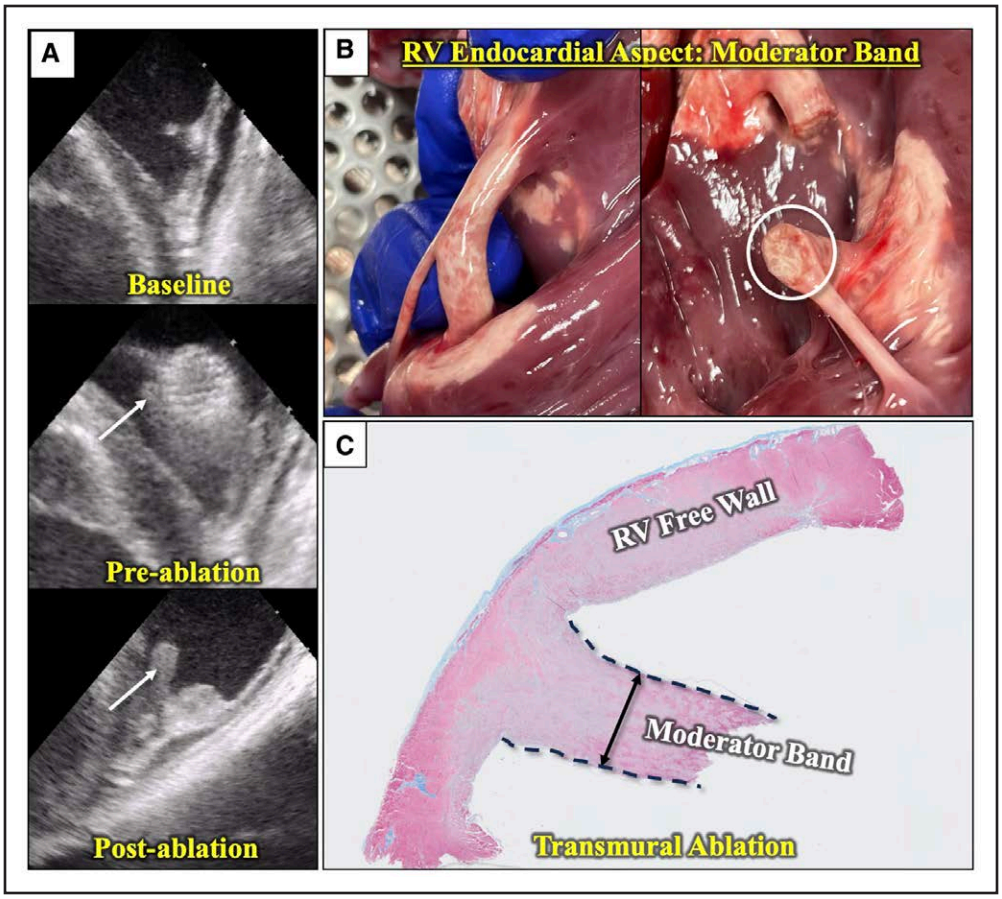

Figure 3. Moderator band ablation.
A, Intracardiac echocardiography images demonstrate the moderator band (MB) at baseline, preablation with the catheter in position, and postablation changes 10 minutes after. The white arrow points to the MB branch in contact with the catheter tip. **B**, Necropsy findings 2 days after ablation show transmural ablation of the MB as well as ablation of insertion points. **C**, Histology confirms transmural ablation of the MB (dotted lines) and the neighboring right ventricular (RV) wall. Masson Trichrome staining.

Statistical Analysis

Categorial variables are displayed as count and percentage. Continuous variables are given as mean±SD if normally distributed, or as median (range) otherwise. Variables were tested for normal distribution via Kolmogorov-Smirnov test. Categorial variables were compared via Fishers exact test, and for comparisons of continuous parameters, Student *t* test or Mann-Whitney *U* test were used depending on the distribution of measurements. To compare paired data, a paired *t* test or Wilcoxon test was used. Two-sided $P<0.05$ were considered statistically significant. All statistical analyses were performed in SPSS 29.0 (IBM Corp, Armonk, NY).

RESULTS

The animal weight at the time of ablation was 59.6±3.4 kg (n=14) and increased to 61.6±4.5 kg ($P=0.03$) after completion of survival. The survival period was completed in 13 of 14 (93%) animals: 1 swine intended for 7-day survival expired 1 day after ablation. In this swine, during an otherwise uneventful procedure, reintubation had been necessary due to a defective endotracheal tube. Necropsy of this swine revealed no unexpected findings other than a small hemorrhagic area within the trachea. Malignant arrhythmia after ventricular ablation or aspiration during reintubation were deemed as possible causes of death. Lesions from this animal were excluded from the analysis.

All other animals completed the survival period without significant events. Transatrial epicardial access was performed in 7 animals (5 with CO_2 insufflation, 2 with saline injection), and subsequent subxiphoid access was successful in all 7 (100%) cases. This was performed after full therapeutic heparinization. In 3 of 7 animals (43%), only mild hemorrhagic staining of the pericardial fluid (light pink) was noted after epicardial access, and no further increase in the bleeding occurred during the procedure. During necropsy, 5 of these 7 (71%) animals showed minimal pericardial effusion and minor adhesions. The perforation site in the right atrial appendage could be identified on the epicardial side as small defect or as an area of intramural hemorrhage in 5 of 7 (71%) swine. The remaining 2 swine had a normal appearing epicardial surface. The perforation site was not visualized within the trabeculated endocardial surface in any of the 7 swine. No other complications were observed.

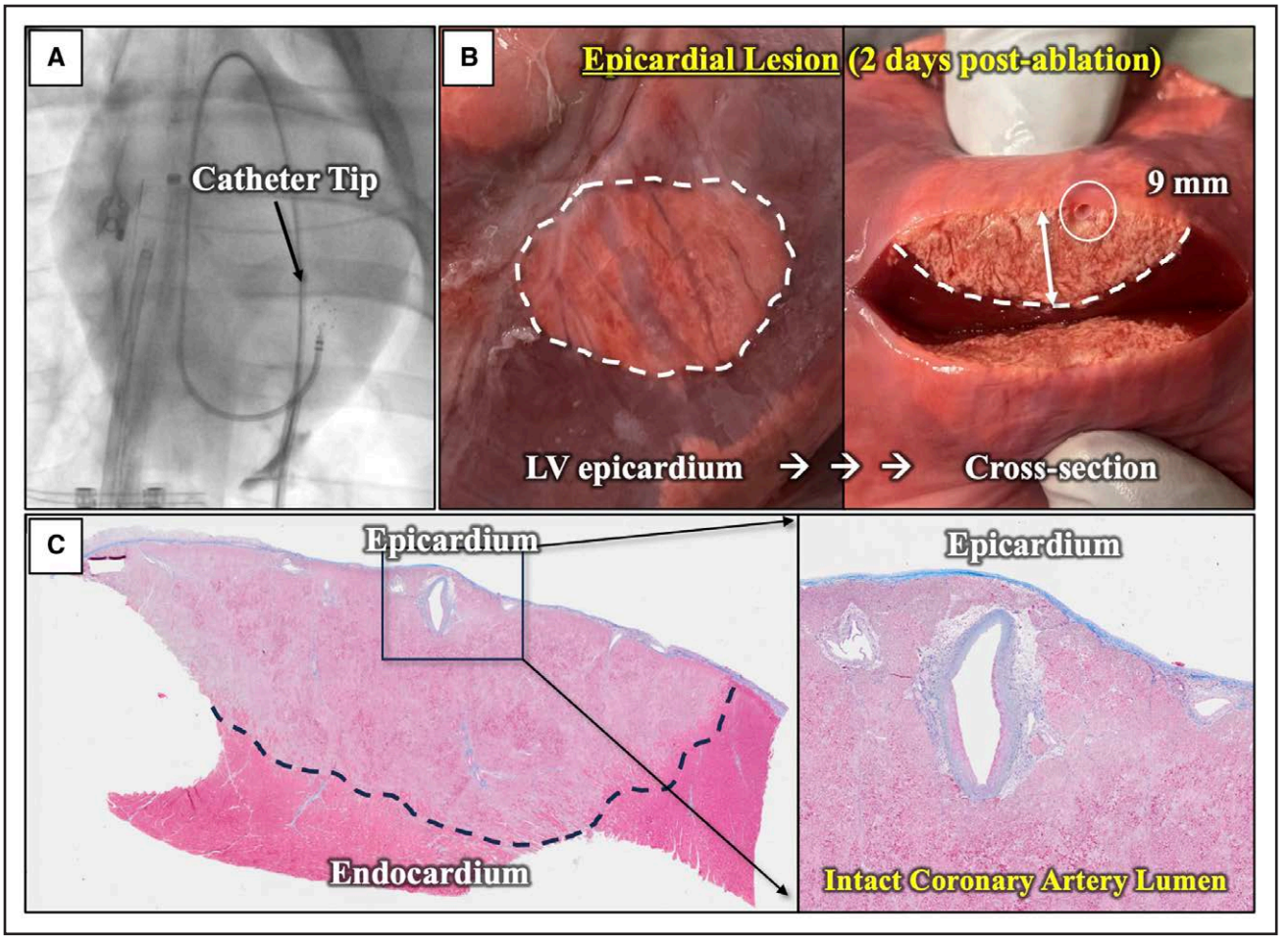

Figure 4. Epicardial monopolar ablation.
A, Fluoroscopic image of the catheter tip (black arrow) on the epicardial surface. Small region of contrast staining seen related to subxiphoid needle epicardial access. **B**, Necropsy findings 2 days after ablation. A wide, homogenous lesion is seen on the epicardial surface (**left**). Cross section (**right**) reveals a lesion depth of 9 mm. Note the large epicardial coronary artery branch within the ablation lesion (white circle). **C**, Histology (Masson Trichrome) demonstrating a homogenous lesion (**left**). The coronary artery lumen remains patent as shown in the zoomed inset (**right**). Note part of the arterial medial wall is ablated as well. LV indicates left ventricle.

Table 1 summarizes the distribution of swine, survival times and various lesion sets. A total of 45 applications were delivered in all 13 swine, and all 45/45 (100%) delivered applications were identified as lesions on necropsy.

Intracavitary Structure Ablation

PM Ablation

In total, 13 PMs (5 anterior LV, 6 posterior LV, 2 RV) were targeted in 7 animals using 3 to 5 repeat applications. Of these, 9 of 13 lesions were assessed at 2 days, 2 of 13 at 7 days, and the remaining 2 of 13 at 21 days. Stable contact between catheter tip and myocardium was identified by ICE for 9 of 13 ablations, and intermittent contact was noted for the remaining 4 of 13 (Figure 1). During PFA applications, rapid myocardial activation/contraction was noted on ICE which, based on visual assessment enhanced the degree of contact between the study catheter and the PM. Clear echogenic changes at ablated sites were noted within minutes after ablation on ICE and became more distinct and prominent over the remaining course of the procedure (Figure 1A). In the 2-day survival cohort, lesions demonstrated superficial and focal hemorrhage centrally (Figure 1B), but this appearance was noted to be absent in the 7-day survival cohort, suggesting resolution. In the chronic 21-day survival cohort, the lesions had a homogeneous, fibrotic appearance. All chordae remained intact, and ICE assessment demonstrated no evidence of mitral valve dysfunction/regurgitation (Figure 1C). On histology (Figure 1B), lesions showed evidence of homogeneous ablation with minimal hemorrhage and moderate inflammation.

For the 9 of 13 lesions with good contact, lesion length, width, and depth were 18.3±2.4, 15.3±1.5, and 5.8±1.0 mm, respectively. Lesions with intermittent contact were significantly shallower (3.9±1.3 mm; P=0.014) but with no significant differences in lesion length and width (18.8±4.7 mm; P=0.78 and 12.7±3.9

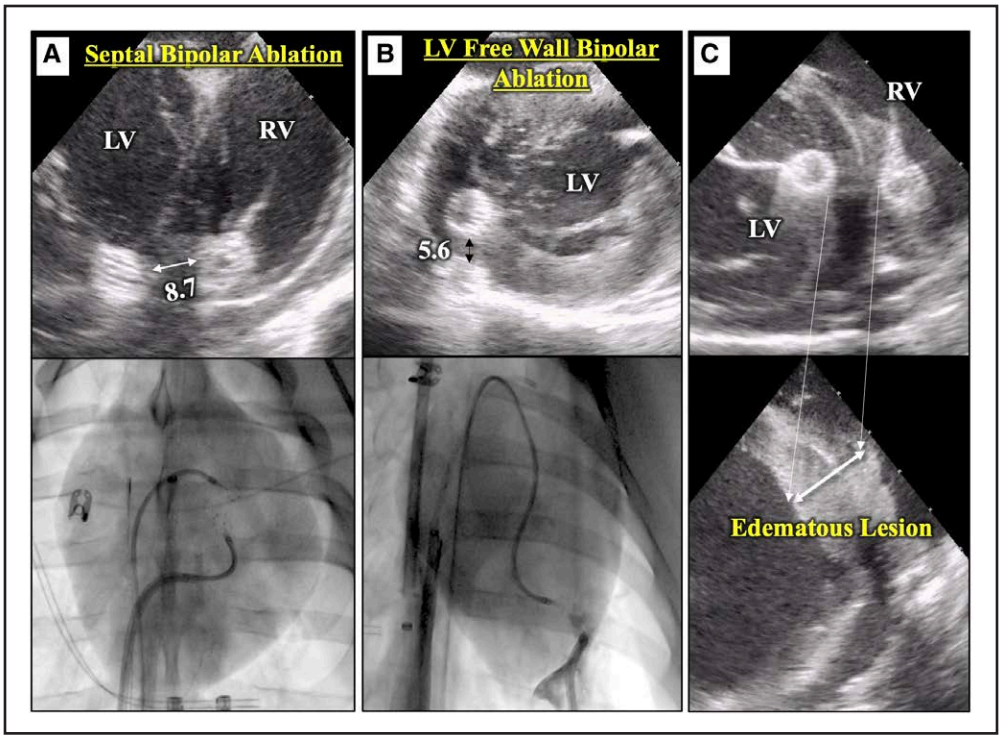

Figure 5. Bipolar ablation–intracardiac echocardiography (ICE) and fluoroscopic views.
A, Septal bipolar ablation. Catheter tips are placed on opposing sites of the interventricular septum and positioned with optimized contact with 8.7-mm separation on ICE (**top**). The corresponding fluoroscopy image is shown in the bottom (AP-view). **B**, Bipolar ablation of the left ventricular (LV) free wall: One catheter tip was introduced retrogradely into the LV, and the other is in the epicardial space. **Top**, ICE view with the catheter tips 5.6 mm separated. The corresponding fluoroscopy image is shown in the bottom. **C**, ICE images during (**top**) and after septal bipolar ablation (**bottom**), showing increased echogenicity and edematous swelling (double arrow) of the ablated tissue. RV indicates right ventricle.

mm; P=0.10, respectively). Lesions with good and stable contact were confined to the PM, without involvement of neighboring myocardium whereas lesions with intermittent contact demonstrated limited extension to myocardial areas around the targeted PM (Figure 2). An overview of all PM lesions assessed after 2 days is presented in Figure S1.

Moderator Band Ablation

The moderator band was targeted in 2 swine. In both cases, contact between the catheter tip and moderator band was assessed by ICE, but given the narrow width of the band and variability of contact, we chose to deliver 3 and 5 applications in the 2 swine. As with the PM lesions, echogenic changes, and evidence of tissue swelling were easily appreciated on ICE (Figure 3A). After survival for 2 days, both lesions demonstrated transmural ablation of the moderator band (confirmed on histology, Figure 3B and 3C) with extension to the septal and lateral RV wall at its insertion. Lesion dimensions along the moderator bands were 19.5 and 24.0 mm (length), 15.3 and 13.5 mm (width), and 5.1 and 6.1 mm (depth). The latter lesion with the 6.1 mm depth, which was placed on the lateral insertion of the moderator band, was noted to have achieved transmural ablation of the RV wall as well.

Epicardial and Bipolar Ablation

Epicardial Ablation

Twelve epicardial monopolar ablation lesions (5 anterior LV, 4 lateral LV, 1 apical LV, 1 posterior LV, and 1 inferior RV) were created in 4 swine that completed their 2-day survival. Two lesions were aborted after the first application due to (1) the induction of ventricular fibrillation (VF), which was noted immediately after pulse delivery and (2) significant sinus bradycardia. There were no ST segment changes noted after these 2 events and the VF event resolved after defibrillation with no further ventricular arrhythmias. The remaining 10 of 12 lesions were delivered with 4 to 5 repetitions of the 5.5-second dose. Catheter placement for ablation and representative images of an epicardial lesion are shown in Figure 4. The catheter was easily manipulated within the pericardial space and contact was readily accomplished given the size of the catheter tip and lack of effusion. Two of the 10 lesions (20%, 1 inferior RV, 1 apical LV) were noted to be transmural in extent. Furthermore, 2 lesions also revealed grossly visible coronary artery branches within the lesions, and their lumen was noted to be preserved (Figure 4B). Of note, there was no evidence of ST segment elevation (with respect to epicardial coronary artery

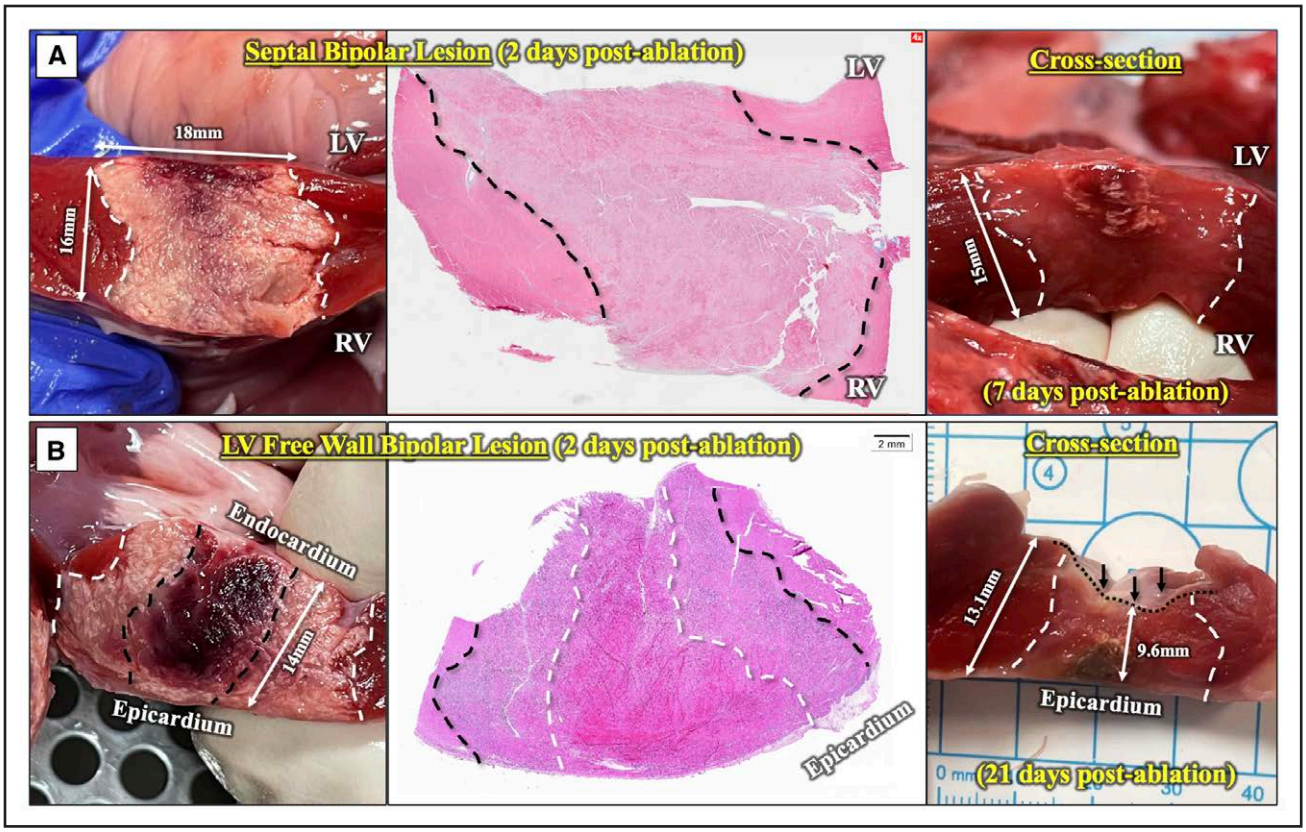

Figure 6. Bipolar ablation–pathology.
A, **Left**, Gross appearance 2 days post-ablation. Septal bipolar lesion (white dotted line) shows central hemorrhagic changes extending to the center on the left ventricular (LV) aspect. This lesion measures 18 mm wide and 16 mm deep. **Middle**, Histology (H&E-stain) demonstrates the septal lesion (black dotted line). **Right**, Gross appearance 7 days post-ablation: a transmural septal lesion demonstrates mild hemorrhage and surrounding calcification limited to the LV aspect, with the rest of the lesion appearing pale typical of chronic PFA lesions. There were no signs of tissue disruption. **B**, **Left**, Gross appearance 2 days post-ablation. A bipolar LV free wall lesion with a central dark area (black dotted line) spanned through the entire thickness that corresponds to transmural hemorrhagic changes in histology (mid, H&E-stain). **Right**, Gross appearance 21 days post-ablation. A transmural LV wall bipolar lesion (white dotted line) is seen with a fibrotic appearance and without signs of hemorrhage. Compared with the neighboring unablated LV free wall (13.1 mm), the lesion center demonstrates reduced wall thickness (9.6 mm) related to wall thinning from fibrotic remodeling. RV indicates right ventricle.

spasm) at any time after completion of these lesions. The lesion that resulted in VF was noted to be at the lateral LV, and no major coronary arteries were noted on necropsy within the lesion. On histology, the epicardial lesions showed evidence of homogeneous ablation with minimal hemorrhage and moderate inflammation. Sparing of the blood vessels within the lesions was seen (Figure 4C). Completed epicardial lesions had a mean length, width, and depth of 30.4±4.2, 23.5±4.1 and 9.1±1.9 mm, respectively.

Bipolar Ablation

Eighteen successful bipolar ablations were delivered in 8 swine: 11 across the interventricular septum (RV to LV septum) and 7 across the LV free wall (LV endocardium to epicardium). Of these, 3 deliveries were aborted prematurely due to the induction of atrioventricular-block (at basal septal locations) in 1 swine, or induction of VF (2 swine). For the remaining 15 of 18 lesions that were completed, a median of 6 (4–7) repeat applications (5.5-second dose) were delivered. Six of 8 swine were survived for 2 days, 1 for 7 days, and 1 for 21 days.

Of the 15 complete deliveries, 2 septal ablations performed within 1 cm from the aortic cusp resulted in complete heart block that was noted only after the last bipolar application. One of these events resolved rapidly and the other required transient ventricular pacing followed by dopamine support until resolution of atrioventricular block (34 minutes post-ablation). Due to changes in lesion size after fibrotic remodeling, the 3/15 bipolar lesions assessed after 21 days were treated as a separate group for dimensional analyses. The remaining 12/15 bipolar lesions had a mean length, width, and depth of 29.6±5.5, 21.0±7.3, and 14.3±4.7 mm, respectively (Figure 6).

Compared with epicardial monopolar lesions, bipolar lesions were significantly deeper (14.3±4.7 versus 9.1±1.9 mm; P=0.001), but there were no significant differences in lesion length (29.6±5.5 versus 30.4±4.2 mm; P=0.66) or width (21.0±7.3 versus 23.5±4.1 mm;

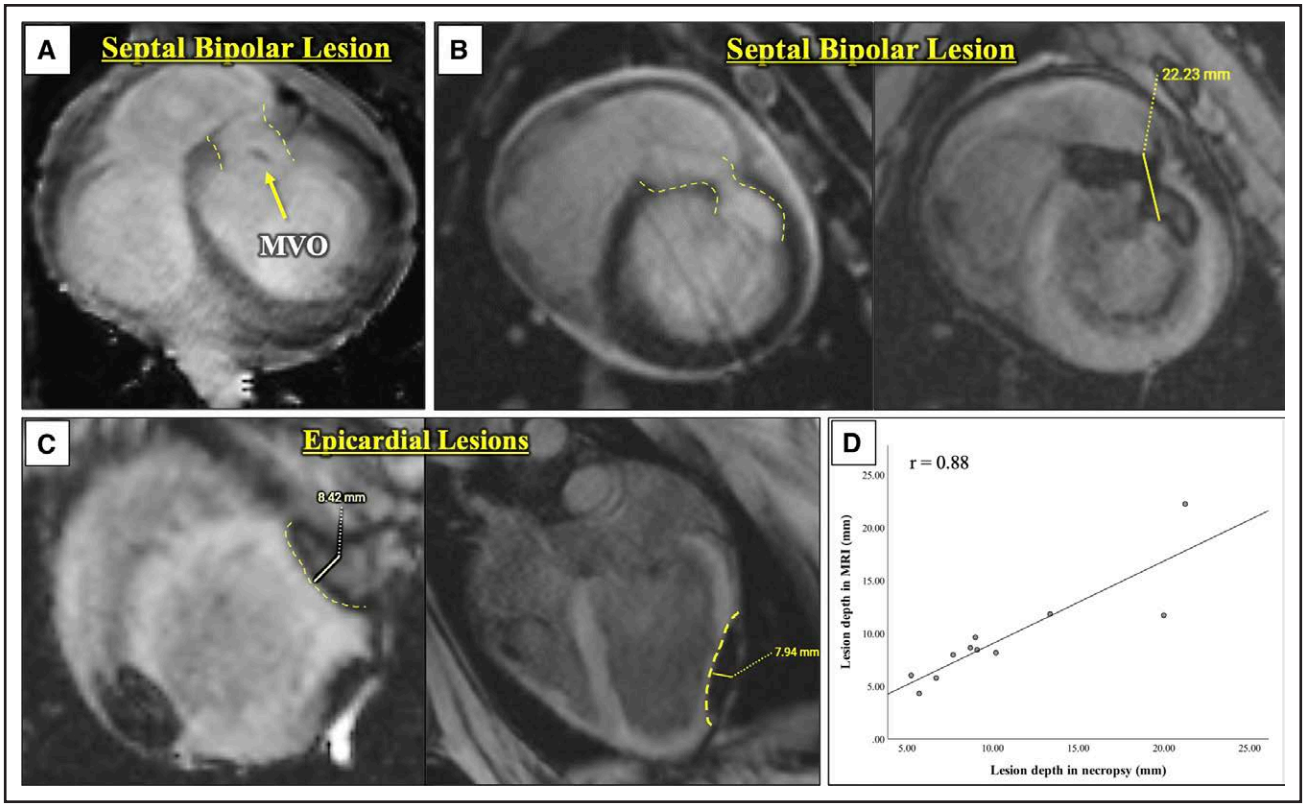

Figure 7. Magnetic resonance imaging.
A, Bright-blood late gadolinium enhancement (LGE) sequence of a septal bipolar lesion. The ablation lesion (yellow dotted line) is well demarcated by LGE, with a small region of microvascular obstruction (MVO, arrow). **B**, Septal bipolar lesion (yellow dotted line) in bright- and dark-blood LGE-sequences. **C**, Epicardial lesions (yellow dotted lines). **D**, Strong correlation (r=0.88) of lesion depth measured in magnetic resonance imaging (MRI) to that measured on necropsy.

P=0.23; Table 2; Figure 8). In the 1 animal that was survived for 21 days, all 3 bipolar LV lesions were transmural. The ablated tissue appeared fibrotic, with reduced ventricular wall thickness, as expected with the contraction inherent to fibrotic remodeling (Figure 6B). Specifically, for these 3 LV lesions, the comparative wall thickness in the lesion center versus the neighboring healthy myocardium were 6.4 and 9.7 mm (33% wall thinning), 9.6 and 13.1 mm (27% wall thinning), and 7.3 and 12.2 mm (40% wall thinning), respectively. There were no signs of aneurysm formation, or areas of tissue disruption or liquefactive necrosis (Figure 6B).

Of the 15 completed bipolar lesions, 13 (87%) were transmural (versus 20% for the epicardial monopolar lesions; *P*=0.002). The deepest transmural lesion had a depth of 21.3 mm. Transmural bipolar lesions typically showed a rectangular cross section while nontransmural lesions appeared semicircular, resembling focal PFA lesions. Of note, 1 incomplete lesion was transmural with only 1 application delivered, spanning through a 11.1-mm thick septum.

Bipolar lesions at the 2-day time point had noticeable hemorrhagic changes in the center of the lesions that either spanned across the entire lesion (after LV free wall

Table 1. Summary of Animals, Survival Periods, and Ablation Details

Survival period	2 days	7 days	21 days
No. of swine	10	2 (one swine expired 1 d post-ablation)	2
Ablation targets	MB (2) RV PM (2) LV anterior PM (3) LV posterior PM (4) Bipolar septal (9) Bipolar LV (4) epicardial LV (11) epicardial RV (1)	LV anterior PM (1*) LV posterior PM (1*) Bipolar septal (2*)	LV anterior PM (1) LV posterior PM (1) Bipolar LV (3)

LV indicates left ventricle; MB, moderator band; PM, papillary muscle; and RV, right ventricle.
*Marks the ablation targets for the animal that completed the 7-d survival period. The numbers in brackets represent the number of lesions created for the ablation targets.

Table 2. Comparison of Lesion Dimensions Achieved With Different Ablation Strategies

	Epicardial	Bipolar	*P* value
Lesions	10 (9 LV, 1 RV)	15 (9 septal, 6 LV)	
Dose	5.5-second repeats	5.5-second repeats	
Length	30.4±4.2 mm	29.6±5.5 mm (n=12)*	0.66
Width	23.5±4.1 mm	21.0±7.3 mm (n=12)*	0.23
Depth	9.1±1.9 mm	14.3±4.7 mm (n=12)*	0.001
Transmurality	2/10 (20%)	13/15 (87%)	0.002

LV indicates left ventricle; and RV, right ventricle.
*Marks the analyses, which excluded the three 21-d lesions that demonstrated scar contraction.

ablation; Figure 6B) or was more prominent at 1 surface (after septal ablation; Figure 6A). Histology confirmed wide, transmural lesions after bipolar ablation. Despite minimal to mild hemorrhagic areas in septal bipolar lesions, the blood vessels within the lesion had patent lumen (Figure S2A). On the other hand, a single LV free wall lesion that was submitted for histology (Figure S2B) revealed both prominent hemorrhage, and vessels with clear ablation of the medial wall but with preservation of their lumen. In the 2 swine that were sacrificed after 7 and 21 days, no significant hemorrhage was noted upon gross observation.

Magnetic Resonance Imaging

All 11/11 lesions delivered were visualized in the 2 swine that underwent cardiac MRI. Ablation lesions demonstrated intense late gadolinium enhancement. Dark-blood sequences facilitated the identification of the endocardial border and lesion boundaries, as has been described for PFA lesions before (Figure 7).[24] In only 1 septal bipolar lesion, an area without contrast enhancement was observed in the lesion center, suggesting microvascular obstruction (Figure 7A). The median lesion depths on MRI and necropsy were 8.4 (4.3–22.2) and 9.0 (5.3–21.3) mm, respectively. Lesion depths on MRI and necropsy correlated strongly (r=0.88; $P<0.001$; Figure 7D).

DISCUSSION

This in vivo evaluation offers additional new insights into the behavior of PFA delivered by the lattice-tip catheter into porcine ventricular myocardium that adds to our prior work. Specifically, we demonstrate that:

1. PMs can be successfully ablated with lesion depths of ≈6 mm using 3 to 5 repeated deliveries of the monopolar 5.5-second PF dose. Poor contact lesions were shallower, and chronic lesions demonstrated fibrotic healing without damage to chordal structures and without mitral regurgitation.
2. Similarly, moderator bands, despite their narrow width and accentuated mobility, can be successfully and transmurally ablated using the repeated 5.5-second PF applications.
3. Transatrial insufflation of carbon dioxide or saline through the distal right atrial appendage can be used to assist epicardial access without incurring significant pericardial bleeding despite its performance on full therapeutic anticoagulation.
4. Epicardial monopolar PFA can create large lesions with a mean length, width, and depth of 30.4±4.2, 23.5±4.1, and 9.1±1.9 mm, respectively also using repeated deliveries of the 5.5-second PF dose.
5. Bipolar PFA lesions were successfully created using 2 separate lattice-tip catheters. The ability to position and maintain stability with this tip allowed for use of repeated 5.5-second applications to create lesions both across the septum and the LV free wall. An 87% transmurality rate and mean depth of 14.3±4.7 mm was achieved without evidence of thermal injury or tissue disruption and with evidence of fibrotic healing.

Several preclinical reports have raised considerable interest in PFA's potential for ventricular ablation, hoping to mirror some of the efficiencies and safety advantages that have been realized for atrial fibrillation ablation with PFA.[21,32–34] We and others previously demonstrated that endocardial ventricular lesions can be created using the

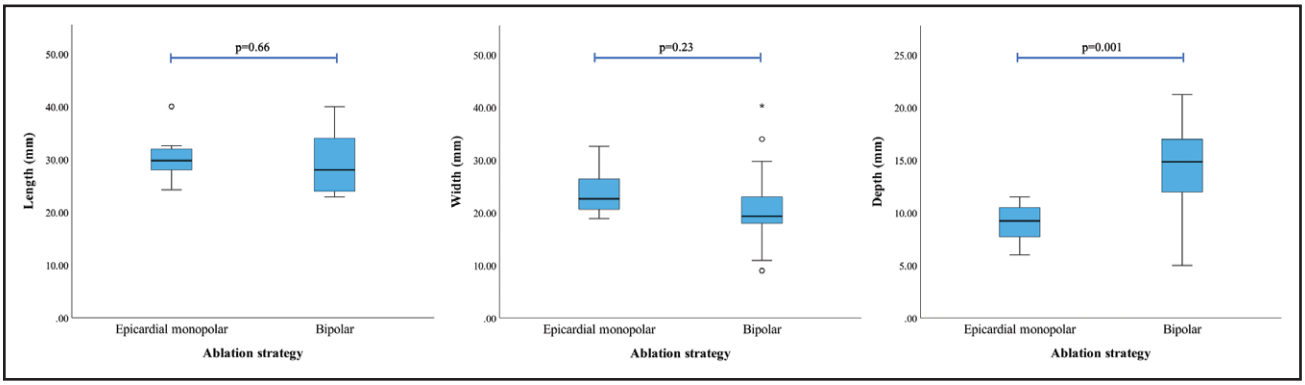

Figure 8. Lesion dimensions with different ablation strategies.
Box plots illustrate the differences in lesion size. Bipolar lesions were significantly deeper than epicardial monopolar lesions, but there were no significant differences in lesion length or width.

lattice-tip PFA catheter and that (1) monopolar applications of 5.5-second duration when repeated can progressively increase lesion dimensions, reaching depths of up to 6.1±2.1 mm (4× repetitions), (2) that epicardial monopolar PFA is feasible, and (3) that endocardial scar (to a maximum depth of 4.2 mm) does not impair PFA lesion formation and penetration.[23] In addition, preclinical evaluations with this and other PFA technologies have corroborated these observations, but the maximum depth achieved has been limited to the ≈6 to 8 mm range across technologies.[22–24,35,36]

Our continued inability to address certain ventricular arrhythmias clinically has long been recognized, and this recently has led to clinical reports of PFA optimized for atrial ablation being used for refractory ventricular arrhythmias with understandably less-than-optimal success.[26,28,29] Thus, approaches to improve depth, workflow efficiency, and ablation outcomes for arrhythmias from different ventricular locations are needed and if and how this can be achieved with PFA remains unexplored.

Our current report demonstrates that PFA is indeed suitable for ablating mobile intracavitary structures. Although stable contact is needed for maximizing depth, the electric-field intensity-based mechanism of PFA, and the design advantages of the lattice-tip structure allowed for consistent lesion formation with ease. This advantage of using PFA with such a tip is especially relevant for PM and moderator band arrhythmias.[6,9,37,38] We demonstrate that PM tips (generally the most unstable regions for catheter placement) as well as other regions (eg, PM base) can be targeted with clinically meaningful lesion depths. Also, after weeks of survival, there appears to be no evidence of disruption of muscular and chordal structures or development of mitral regurgitation. The ability to completely ablate the moderator band and its insertion site is particularly notable as these are notoriously difficult sites to ablate with conventional catheters.

The epicardial lesions created in this report were noted to be significantly larger and deeper (≈9 mm versus ≈6–7 mm) than endocardial lesions that have been described.[23,35] Factors favoring improved depth in the epicardium include improved and more stable contact within the confined pericardial space that naturally promotes epicardial contact with the large compressible lattice tip and the lack of blood pool–related loss of current during PFA applications. Although we did encounter occasional instances of VF, this phenomenon is consistent with the stimulatory nature of PFA as we have demonstrated in our prior reports. However, it is also important to recognize the strong proclivity for developing VF during ventricular ablation in swine, a phenomenon that is widely appreciated with radiofrequency ablation as well.[23] The clinical relevance of this event and the need for ventricular gating remains to be determined.

Based on the efficacy of bipolar radiofrequency ablation as a solution for deep myocardial substrates, we also investigated bipolar PFA delivered across 2 catheter tips using this system.[15] We successfully created transmural lesions (14.3±4.7 mm) across the septum and LV free wall for 87% of completed deliveries, suggesting that this is a highly efficacious approach. However, there are several important aspects to consider. This approach creates the deepest lesion with any PFA catheter thus far. The occurrence of prominent hemorrhagic changes is significant as the delivered current between 2 catheters with good/symmetrical contact can concentrate the electric-field intensity. It is possible that these high fields are responsible for the degree of hemorrhage (typically not seen with this catheter/waveform during monopolar applications), as well as the corresponding small region of microvascular obstruction noted on MRI. In addition, we did not measure the temperature profile of such bipolar deliveries, and while we estimate thermal ablation to be unlikely, it cannot be ruled out.

The shape of the bipolar lesion was cylindrical when the catheters were directly opposite each other with intercatheter distances of ≈10 to 15 mm. As the separation increased, the lesions appeared to adopt semicircular shapes reminiscent of how radiofrequency current behaves when delivered in bipolar fashion with increasing separation. However, transmurality was observed in 1 lesion despite ≈21 mm of separation (although in a relatively narrow region), and in another instance, a single bipolar application alone was able to achieve transmurality across 11 mm thick myocardium. Further studies are needed to understand the minimum number of repeat applications needed for transmurality and at what separation loss of transmurality consistently occurs. The occurrence of atrioventricular block at basal septal sites, albeit reversible, is also important to consider as this effect is likely to be clinically relevant and appropriate care must be taken to address such an occurrence even if transient. Furthermore, a better understanding of how far from the conduction system PFA deliveries can be safely administered is needed.

We previously reported the occurrence of edema after PFA in swine atria; as demonstrated in this report, edema occurs in the ventricle as well.[30] The impact of large lesions and accompanying edema must be taken into consideration as the consequent impact of wall motion abnormalities can have adverse hemodynamic effects—particularly in patients with either reduced ventricular function or in instances wherein a significant volume of healthy myocardium is targeted (more prone to edema). Finally, at necropsy, the 2 animals with bipolar lesions that were survived for >48 hours showed firm, contracted regions of scarring with calcification but without evidence of tissue disruption, liquefactive necrosis or aneurysmal change. This is important as ventricular septal defects have been reported with bipolar radiofrequency current; although we are limited by our sample

size, we think (based on this and prior chronic evaluations) that this risk is less likely with PFA. Of course, this must be confirmed with additional experience.

Limitations

This preclinical evaluation was performed in healthy swine, so caution should be exercised in extrapolating these findings to healthy human and scarred myocardium. Individual experiments are of limited sample size given their exploratory nature and this can consequently impact the strength of the observations described. The animals that were survived for >48 hours are limited in this report and this should be considered when extrapolating to long-term lesion healing and behavior. None of the bipolar or epicardial applications involved direct assessment of coronary artery spasm either at the site of application or remotely, so this risk needs to be separately considered.

CONCLUSIONS

Focal PFA using the lattice-tip catheter can reliably create large ventricular lesions with consistency and reasonable safety. We specifically demonstrate successful ablation of intracavitary mobile structures, creation of large and deep epicardial lesions, and dual-catheter transmural bipolar ablation of the septum and the left ventricular wall.

ARTICLE INFORMATION

Received January 24, 2024; accepted April 16, 2024.

Affiliations

Helmsley Electrophysiology Center (M.N., K.W., I.K., V.Y.R., J.S.K.). Atherothrombosis Research Unit, Icahn School of Medicine at Mount Sinai, New York, NY (C.G.S.-G.). Department of Cardiology, University Medical Center Hamburg-Eppendorf, Hamburg, Germany (M.N.).

Sources of Funding

This study was funded by Affera/Medtronic. Dr Nies is supported by the Walter-Benjamin Fellowship from the Deutsche Forschungsgemeinschaft (523496205).

Disclosures

Drs Koruth and Reddy have served as a consultant to and received grant support and equity from Affera-Medtronic. A comprehensive list of all financial disclosures (unrelated to this article) is included in the Supplemental Material. Dr Nies has received a scholarship from the German Research Foundation (Deutsche Forschungsgemeinschaft). The other authors report no conflicts.

Supplemental Material

Figures S1 and S2
Comprehensive list of all financial disclosures

REFERENCES

1. Della Bella P, Baratto F, Tsiachris D, Trevisi N, Vergara P, Bisceglia C, Petracca F, Carbucicchio C, Benussi S, Maisano F, et al. Management of ventricular tachycardia in the setting of a dedicated unit for the treatment of complex ventricular arrhythmias: long-term outcome after ablation. *Circulation*. 2013;127:1359–1368. doi: 10.1161/CIRCULATIONAHA.112.000872
2. Wasmer K, Reinecke H, Heitmann M, Dechering DG, Reinke F, Lange PS, Frommeyer G, Kochhauser S, Leitz P, Eckardt L, et al. Clinical, procedural and long-term outcome of ischemic VT ablation in patients with previous anterior versus inferior myocardial infarction. *Clin Res Cardiol*. 2020;109:1282–1291. doi: 10.1007/s00392-020-01622-z
3. Yamashita S, Cochet H, Sacher F, Mahida S, Berte B, Hooks D, Sellal JM, Al Jefairi N, Frontera A, Komatsu Y, et al. Impact of new technologies and approaches for post-myocardial infarction ventricular tachycardia ablation during long-term follow-up. *Circ Arrhythm Electrophysiol*. 2016;9:e003901. doi: 10.1161/CIRCEP.116.003901
4. Barkagan M, Leshem E, Shapira-Daniels A, Sroubek J, Buxton AE, Saffitz JE, Anter E. Histopathological characterization of radiofrequency ablation in ventricular scar Tissue. *JACC Clin Electrophysiol*. 2019;5:920–931. doi: 10.1016/j.jacep.2019.05.011
5. Schwartzman D, Chang I, Michele JJ, Mirotznik MS, Foster KR. Electrical impedance properties of normal and chronically infarcted left ventricular myocardium. *J Interv Card Electrophysiol*. 1999;3:213–224. doi: 10.1023/a:1009887306055
6. Latchamsetty R, Yokokawa M, Morady F, Kim HM, Mathew S, Tilz R, Kuck KH, Nagashima K, Tedrow U, Stevenson WG, et al. Multicenter outcomes for catheter ablation of idiopathic premature ventricular complexes. *JACC Clin Electrophysiol*. 2015;1:116–123. doi: 10.1016/j.jacep.2015.04.005
7. Rivera S, Ricapito Mde L, Tomas L, Parodi J, Bardera Molina G, Banega R, Bueti P, Orosco A, Reinoso M, Caro M, et al. Results of cryoenergy and radiofrequency-based catheter ablation for treating ventricular arrhythmias arising from the papillary muscles of the left ventricle, guided by intracardiac echocardiography and image integration. *Circ Arrhythm Electrophysiol*. 2016;9:e003874. doi: 10.1161/CIRCEP.115.003874
8. Mariani MV, Piro A, Magnocavallo M, Chimenti C, Della Rocca D, Santangeli P, Natale A, Fedele F, Lavalle C. Catheter ablation for papillary muscle arrhythmias: a systematic review. *Pacing Clin Electrophysiol*. 2022;45:519–531. doi: 10.1111/pace.14462
9. Yokokawa M, Good E, Desjardins B, Crawford T, Jongnarangsin K, Chugh A, Pelosi F Jr, Oral H, Morady F, Bogun F. Predictors of successful catheter ablation of ventricular arrhythmias arising from the papillary muscles. *Heart Rhythm*. 2010;7:1654–1659. doi: 10.1016/j.hrthm.2010.07.013
10. Inoue H, Waller BF, Zipes DP. Intracoronary ethyl alcohol or phenol injection ablates aconitine-induced ventricular tachycardia in dogs. *J Am Coll Cardiol*. 1987;10:1342–1349. doi: 10.1016/s0735-1097(87)80139-0
11. Brugada P, de Swart H, Smeets JL, Wellens HJ. Transcoronary chemical ablation of ventricular tachycardia. *Circulation*. 1989;79:475–482. doi: 10.1161/01.cir.79.3.475
12. Sharma A, Wong D, Weidlich G, Fogarty T, Jack A, Sumanaweera T, Maguire P. Noninvasive stereotactic radiosurgery (CyberHeart) for creation of ablation lesions in the atrium. *Heart Rhythm*. 2010;7:802–810. doi: 10.1016/j.hrthm.2010.02.010
13. Loo BW Jr, Soltys SG, Wang L, Lo A, Fahimian BP, Iagaru A, Norton L, Shan X, Gardner E, Fogarty T, et al. Stereotactic ablative radiotherapy for the treatment of refractory cardiac ventricular arrhythmia. *Circ Arrhythm Electrophysiol*. 2015;8:748–750. doi: 10.1161/CIRCEP.115.002765
14. Timmermans C, Manusama R, Alzand B, Rodriguez LM. Catheter-based cryoablation of postinfarction and idiopathic ventricular tachycardia: initial experience in a selected population. *J Cardiovasc Electrophysiol*. 2010;21:255–261. doi: 10.1111/j.1540-8167.2009.01610.x
15. Koruth JS, Dukkipati S, Miller MA, Neuzil P, d'Avila A, Reddy VY. Bipolar irrigated radiofrequency ablation: a therapeutic option for refractory intramural atrial and ventricular tachycardia circuits. *Heart Rhythm*. 2012;9:1932–1941. doi: 10.1016/j.hrthm.2012.08.001
16. Nguyen DT, Tzou WS, Sandhu A, Gianni C, Anter E, Tung R, Valderrabano M, Hranitzky P, Soeijma K, Saenz L, et al. Prospective multicenter experience with cooled radiofrequency ablation using high impedance irrigant to target deep myocardial substrate refractory to standard ablation. *JACC Clin Electrophysiol*. 2018;4:1176–1185. doi: 10.1016/j.jacep.2018.06.021
17. Turagam MK, Neuzil P, Schmidt B, Reichlin T, Neven K, Metzner A, Hansen J, Blaauw Y, Maury P, Arentz T, et al. Safety and effectiveness of pulsed field ablation to treat atrial fibrillation: one-year outcomes from the MANIFEST-PF registry. *Circulation*. 2023;148:35–46. doi: 10.1161/circulationaha.123.064959
18. Duytschaever M, De Potter T, Grimaldi M, Anic A, Vijgen J, Neuzil P, Van Herendael H, Verma A, Skanes A, Scherr D, et al; inspIRE Trial Investigators. Paroxysmal atrial fibrillation ablation using a novel variable-loop biphasic pulsed field ablation catheter integrated with a 3-dimensional mapping system: 1-year outcomes of the multicenter inspIRE study. *Circ Arrhythm Electrophysiol*. 2023;16:e011780. doi: 10.1161/CIRCEP.122.011780

19. Schmidt B, Bordignon S, Tohoku S, Chen S, Bologna F, Urbanek L, Pansera F, Ernst M, Chun KRJ. 5S study: safe and simple single shot pulmonary vein isolation with pulsed field ablation using sedation. *Circ Arrhythm Electrophysiol*. 2022;15:e010817. doi: 10.1161/CIRCEP.121.010817
20. Reddy VY, Gerstenfeld EP, Natale A, Whang W, Cuoco FA, Patel C, Mountantonakis SE, Gibson DN, Harding JD, Ellis CR, et al; ADVENT Investigators. Pulsed field or conventional thermal ablation for paroxysmal atrial fibrillation. *N Engl J Med*. 2023;389:1660–1671. doi: 10.1056/NEJMoa2307291
21. Koruth JS, Kuroki K, Iwasawa J, Viswanathan R, Brose R, Buck ED, Donskoy E, Dukkipati SR, Reddy VY. Endocardial ventricular pulsed field ablation: a proof-of-concept preclinical evaluation. *Europace*. 2020;22:434–439. doi: 10.1093/europace/euz341
22. Im SI, Higuchi S, Lee A, Stillson C, Buck E, Morrow B, Schenider K, Speltz M, Gerstenfeld EP. Pulsed field ablation of left ventricular myocardium in a swine infarct model. *JACC Clin Electrophysiol*. 2022;8:722–731. doi: 10.1016/j.jacep.2022.03.007
23. Kawamura I, Reddy VY, Wang BJ, Dukkipati SR, Chaudhry HW, Santos-Gallego CG, Koruth JS. Pulsed field ablation of the porcine ventricle using a focal lattice-tip catheter. *Circ Arrhythm Electrophysiol*. 2022;15:e011120. doi: 10.1161/CIRCEP.122.011120
24. Kawamura I, Reddy VY, Santos-Gallego CG, Wang BJ, Chaudhry HW, Buck ED, Mavroudis G, Jerrell S, Schneider CW, Speltz M, et al. Electrophysiology, pathology, and imaging of pulsed field ablation of scarred and healthy ventricles in swine. *Circ Arrhythm Electrophysiol*. 2023;16:e011369. doi: 10.1161/CIRCEP.122.011369
25. Sandhu U, Alkukhun L, Kheiri B, Hodovan J, Chiang K, Splanger T, Castellvi Q, Zhao Y, Nazer B. In vivo pulsed-field ablation in healthy vs. chronically infarcted ventricular myocardium: biophysical and histologic characterization. *Europace*. 2023;25:1503–1509. doi: 10.1093/europace/euac252
26. Krause U, Bergau L, Zabel M, Muller MJ, Paul TF. pulsed field ablation of ventricular tachycardia in a patient with Ebstein's anomaly. *Eur Heart J Case Rep*. 2023;7:ytad093. doi: 10.1093/ehjcr/ytad093
27. Ouss A, van Stratum L, van der Voort P, Dekker L. First in human pulsed field ablation to treat scar-related ventricular tachycardia in ischemic heart disease: a case report. *J Interv Card Electrophysiol*. 2023;66:509–510. doi: 10.1007/s10840-022-01407-6
28. Lozano-Granero C, Hirokami J, Franco E, Tohoku S, Matia-Frances R, Schmidt B, Hernandez-Madrid A, Zamorano Gomez JL, Moreno J, Chun J. Case series of ventricular tachycardia ablation with pulsed-field ablation: pushing technology further (into the ventricle). *JACC Clin Electrophysiol*. 2023;9:1990–1994. doi: 10.1016/j.jacep.2023.03.024
29. Adragao P, Matos D, Carmo P, Costa FM, Ramos S. Pulsed-field ablation vs radiofrequency ablation for ventricular tachycardia: first in-human case of histologic lesion analysis. *Heart Rhythm*. 2023;20:1395–1398. doi: 10.1016/j.hrthm.2023.07.062
30. Koruth JS, Kuroki K, Kawamura I, Stoffregen WC, Dukkipati SR, Neuzil P, Reddy VY. Focal pulsed field ablation for pulmonary vein isolation and linear atrial lesions: a preclinical assessment of safety and durability. *Circ Arrhythm Electrophysiol*. 2020;13:e008716. doi: 10.1161/CIRCEP.120.008716
31. Reddy VY, Anter E, Rackauskas G, Peichl P, Koruth JS, Petru J, Funasako M, Minami K, Natale A, Jais P, et al. Lattice-tip focal ablation catheter that toggles between radiofrequency and pulsed field energy to treat atrial fibrillation: a first-in-human trial. *Circ Arrhythm Electrophysiol*. 2020;13:e008718. doi: 10.1161/CIRCEP.120.008718
32. Neven K, van Driel V, van Wessel H, van Es R, Doevendans PA, Wittkampf F. Myocardial lesion size after epicardial electroporation catheter ablation after subxiphoid puncture. *Circ Arrhythm Electrophysiol*. 2014;7:728–733. doi: 10.1161/CIRCEP.114.001659
33. Neven K, van Driel V, van Wessel H, van Es R, du Pre B, Doevendans PA, Wittkampf F. Safety and feasibility of closed chest epicardial catheter ablation using electroporation. *Circ Arrhythm Electrophysiol*. 2014;7:913–919. doi: 10.1161/CIRCEP.114.001607
34. Neven K, van Driel V, Vink A, du Pre BC, van Wessel H, Futing A, Doevendans PA, Wittkampf FHM, van Es R. Characteristics and time course of acute and chronic myocardial lesion formation after electroporation ablation in the porcine model. *J Cardiovasc Electrophysiol*. 2022;33:360–367. doi: 10.1111/jce.15352
35. Younis A, Zilberman I, Krywanczyk A, Higuchi K, Yavin HD, Sroubek J, Anter E. Effect of pulsed-field and radiofrequency ablation on heterogeneous ventricular scar in a swine model of healed myocardial infarction. *Circ Arrhythm Electrophysiol*. 2022;15:e011209. doi: 10.1161/CIRCEP.122.011209
36. Yavin HD, Higuchi K, Sroubek J, Younis A, Zilberman I, Anter E. Pulsed-field ablation in ventricular myocardium using a focal catheter: the impact of application repetition on lesion dimensions. *Circ Arrhythm Electrophysiol*. 2021;14:e010375. doi: 10.1161/CIRCEP.121.010375
37. Barber M, Chinitz J, John R. Arrhythmias from the right ventricular moderator band: diagnosis and management. *Arrhythm Electrophysiol Rev*. 2020;8:294–299. doi: 10.15420/aer.2019.18
38. Sadek MM, Benhayon D, Sureddi R, Chik W, Santangeli P, Supple GE, Hutchinson MD, Bala R, Carballeira L, Zado ES, et al. Idiopathic ventricular arrhythmias originating from the moderator band: electrocardiographic characteristics and treatment by catheter ablation. *Heart Rhythm*. 2015;12:67–75. doi: 10.1016/j.hrthm.2014.08.029